

EVOLUTION OF THE PULSATION PROPERTIES OF HOT PRE-WHITE DWARF STARS

STEVEN D. KAWALER

Department of Astronomy, University of Texas at Austin

C. J. HANSEN

Joint Institute for Laboratory Astrophysics, University of Colorado

AND

D. E. WINGET

Department of Astronomy, University of Texas at Austin

Received 1984 November 12; accepted 1985 February 26

ABSTRACT

We have solved the equations of linear, nonradial adiabatic oscillation for evolutionary pre-white dwarf (PWD) models. We have computed periods, eigenfunctions, weight functions, and rates of period change (dP/dt) for high-order dipole and quadrupole gravity mode oscillations in spherical, nonrotating PWD models with $M_* = 0.60-0.95 M_\odot$ and $\log(L/L_\odot) = 3.0-1.0$. The region where the adiabatic periods are determined shifts from within the degenerate core out to the nondegenerate envelope near luminosities of $\log(L/L_\odot) = 2.0$ for $0.60 M_\odot$ models. The pulsation period generally increases with time for $\log(L/L_\odot) < 3.0$. Time scales for period change are comparable to the thermal time scale in the region of maximum weight in the star. For models with luminosities appropriate to the pulsating PG 1159 stars [$\log(L/L_\odot) \sim 2.0$], we find that the e -folding time scales for periods must be less than or of the order of 10^6 years; this time scale is shown to be representative for the general class of cooling PWD models. These results place stringent upper limits on the absolute magnitude of the rates of period change expected in stars represented by this class of models. The recently measured period decrease in the 516 s period of the pulsating star PG 1159-035 is consistent with the limits provided by our results. We note, however, that the observed decrease in the period, as opposed to the increase implied by our models with $\log(L/L_\odot) \sim 2.0$, may indicate the possible importance of other contributions to dP/dt .

Subject headings: stars: pulsation — stars: white dwarfs

I. INTRODUCTION

Over the last five years several extremely hot DO degenerate dwarf stars have been reported to be multiperiodic pulsating variable stars. The first of these was PG 1159-035, initially reported by McGraw *et al.* (1979). Other stars with similar spectra have been found to pulsate with similar periods: PG 1707+427 and PG 2131+066 have periods around 500 s (Bond *et al.* 1984). The surface temperatures of these objects are extremely high, with estimates for PG 1159-035 ranging from 80×10^3 to 150×10^3 K (Wegner *et al.* 1982). Model atmosphere analysis suggests a surface gravity of $7 < \log g < 8$ (Wesemael, Green, and Liebert 1982). Spectroscopically these stars show He II lines in absorption with emission cores and absorption lines of C IV and other heavy elements (Green and Liebert 1979; Sion *et al.* 1985). The lack of surface hydrogen, coupled with high surface gravities, implied an advanced evolutionary state for these pulsating stars. Their approximate location in the H-R diagram between the planetary nebula regime and the white dwarfs suggests that they are most likely rapidly evolving and cooling down into the white dwarf region of the H-R diagram.

The interior structure of pre-white dwarf stars (PWDs) may be inferred from what is known of their possible progenitors and their descendants, the white dwarfs (WDs). One attractive possibility is that the progenitors of the PG 1159 stars are the nuclei of planetary nebulae (PNNs). The evolution of PNNs has been studied from a theoretical standpoint by several investigators (Paczynski 1971; Iben 1982, 1984; Iben and Tutukov 1984; Kovetz and Harpaz 1981; Schönberner 1979,

1981, 1983), but several basic questions remain. PNNs are assumed to be the hot cores of low-mass asymptotic giant branch (AGB) stars which have ejected most of their hydrogen-rich envelopes during the planetary nebula formation phase. By altering the amount of hydrogen and helium-rich material remaining in the envelope following nebula ejection, Iben (1984) demonstrated a variety of evolutionary possibilities. His PNN models go through various phases of shell helium and hydrogen burning before reaching the PWD phase. Schönberner (1979, 1981, 1983) has also followed the evolution of AGB stars by including a Reimers-like stellar wind. A superwind phase is needed to move the model off the AGB and into the PNN region. His models also experience episodes of shell burning following nebular ejection while evolving through the PNN phase to a PWD configuration.

The results of these various investigations of PNN evolution bear a qualitative resemblance to one another as a result of the similarities in the structure of the degenerate cores of the models. Since the thermal time scale of the degenerate core is 10-100 times longer than the e -folding time for luminosity (the evolutionary time scale), this residual thermal structure is retained through the PWD phase. On the other hand, the details of shell flashes and mass loss in the AGB phase, and of nuclear burning on the remnant core, are important for determining the compositional and thermal structure of the outer layers of the PNN model at the approach to the PWD phase. The thermal time scale for these outer layers is of the order of the evolutionary time scale. Therefore, while the pulsation properties of the high-luminosity phases may be sensitive to

the uncertainties of PNN evolution, these uncertainties should diminish in importance (via thermal relaxation) as the model cools.

If the pulsating PG 1159 stars are hot degenerates, then the observed pulsation periods are much longer than the expected radial pulsation period (on the order of the dynamical time scale, or ~ 20 – 50 s). This, along with the multiperiodic nature of their light curves, strongly suggests that they are undergoing nonradial g -mode pulsation. The initial investigations of stellar pulsation in this area, conducted by Starrfield and collaborators (Starrfield *et al.* 1983; Starrfield *et al.* 1984), support this interpretation of the luminosity variations. Their studies, employing static stellar envelopes based on available evolutionary tracks of PNN models, show that partial ionization of oxygen and/or carbon can drive high-overtone nonradial g -modes in the temperature domain of the pulsating PG 1159 stars.

McGraw *et al.* (1979) pointed out that, if PG 1159–035 is indeed a pre-white dwarf star, then its rapid evolutionary changes in structure might be indirectly observable through observations of secular period changes. This suggestion was elaborated upon by Winget, Hansen, and Van Horn (1983, hereafter WHVH), who estimated that pulsating PG 1159 stars should exhibit period changes with e -folding times (τ) of $\sim 10^6$ yr. With such relatively short time scales (by stellar standards) they proposed that τ could be measured over just a few observing seasons. In addition, their preliminary calculations indicated that the rate of change of period (dP/dt) for PG 1159–035 should be negative, that is, its period should be decreasing with time. The recent determination of $dP/dt = (-1.2 \pm 0.1) \times 10^{-11}$ s s $^{-1}$ for the 516 s period of PG 1159 (Winget *et al.* 1985) confirms those expectations.

To take full advantage of this new observational result, we have begun an investigation of the pulsation properties of evolutionary models of cooling PWDs. The purpose of this study is to create a theoretical framework around which we can build up our understanding of the PWD phase of evolution, using the information available from the observations of the PG 1159 stars.

In this first paper we consider simple, purely homogeneous carbon evolutionary sequences evolved from starting models which are the remnants of intermediate-mass stars evolved from the main sequence to the AGB. In view of the uncertainties of PWD structure, we are considering a pure carbon composition to try to isolate the separate factors that could affect the pulsation properties of PWDs. Once the phenomena associated with these simple models are understood, we can then consider how the details of the prior history of PWDs can further affect their nonradial pulsation properties. For this first study we concentrate on mechanical adiabatic motions; it is primarily these which determine the spectrum of possible periods over time.

We find periods that increase with time for models with temperatures and surface gravities appropriate to PG 1159–035. In addition, we have examined some PWD models kindly provided by I. Iben at the University of Illinois. Despite differences in input physics, composition, and treatment of nuclear burning, Iben's models are similar in their pulsation properties to the models presented in this paper, including the sign and magnitude of $d \ln P/dt$. We show that these similarities result from basic similarities of the regions in which the pulsation modes are formed.

In § II we discuss the construction of evolutionary sequences

of 0.60, 0.78, and 0.95 M_{\odot} PWD models. Section III describes the various methods used to calculate and interpret the adiabatic pulsation properties of the evolutionary models. The results of our analysis are presented in § IV. We conclude with a discussion of the observed value of dP/dt for PG 1159–035 (Winget *et al.* 1985) in the context of evolutionary changes in the adiabatic pulsation properties of PWD models. We also note the potential importance of additional effects, not included in this analysis, in understanding measurements of dP/dt .

II. CONSTRUCTION OF THE EVOLUTIONARY MODELS

To study the pulsation properties of PWD models, we require evolutionary models which represent the important physical properties of PWD stars. In particular, models of early PWDs should reflect the thermal structure of their progenitors. That structure determines, to a great extent, the period spectrum. Because of the difficulties and uncertainties in modeling evolutionary histories of stars in their later (and, practically, last) stages, certain assumptions and approximations must be made. Among these is our assumption that the PWD models are assumed to be cooling PNNs that have recently ceased nuclear burning.

To obtain starting models for our PWD evolutionary sequences, we have started with spherical, nonrotating main-sequence models of Population I composition. Using an evolutionary code based on those used by Paczyński (1970, 1974), we have evolved models of 3.00, 4.25, and 5.00 M_{\odot} up into the AGB phase. Once the mass in the shell-burning region became sufficiently small ($< 0.02 M_{\odot}$), we removed most of the convective envelope of the model, comprising roughly 80% of the original stellar mass. Removal of mass from the AGB model was done in stages, with sufficient time allowed for the models to relax thermally following each reduction in mass. Typically, less than 0.01 M_{\odot} of hydrogen remained above the hydrogen shell source. After the preliminary models relaxed to this configuration, nuclear burning was artificially turned off as the models evolved across the PNN regime toward the constant-radius WD cooling track. For a description of the evolution of PNNs in this phase see Schönberner (1983) or Paczyński (1971). Note, however, that the thermal time scale of the degenerate core is sufficiently long that the thermal structure resulting from the prior evolution is "remembered" for long periods of time.

Initial models for the study of PWD evolution were selected from the early parts of this PNN sequence. The core composition of the starting models is about 90% carbon and 10% oxygen. Because of the high energy loss rates from neutrino emission in these hot evolutionary stages, the inner core shows a pronounced temperature inversion. In addition, the 0.60 M_{\odot} model showed a secondary temperature maximum at the position of the helium-burning shell source.

We used an updated version of the Lamb and Van Horn (1975) white dwarf evolution code to follow the subsequent evolution of PWD models that were used in the pulsation study. For the degenerate core this code uses the equation of state described in detail in Lamb (1974). This equation of state accurately treats Coulomb interactions between the ions and electrons, and other nonideal effects important to white dwarf evolution at PWD and later stages. The negative correction to the internal energy due to Coulomb effects increases in magnitude with decreasing temperature and results in the gradual increase in the specific heat of PWD interiors (Lamb 1974;

Lamb and Van Horn 1975). Therefore, with these effects taken into consideration in a self-consistent way, models of PWDs can be expected to cool slightly more slowly than standard PNN (Iben 1984) and PWD (Iben and Tutukov 1984) studies have indicated.

For the envelope, the equation of state is based on that tabulated by Fontaine, Graboske, and Van Horn (1977, hereafter FGVH) for a Weigert V (0.999 ^{12}C) composition. Early in this investigation we found an inconsistency in this equation of state. For the partial ionization of carbon under nondegenerate conditions the FGVH equation of state does not give self-consistent values for interpolated quantities. This results from an ionization stage that apparently was left out of the original FGVH equation of state for carbon partial ionization. In the un-ionized and fully ionized states, as well as under degenerate and partially ionized conditions, the FGVH equation of state is self-consistent. We have recalculated the equation of state in the region of difficulty and incorporated the corrections into the remainder of the FGVH tables. (The corrected tables are available upon request.) Also, the hot envelopes of the PWD models made it necessary to extend the bounds of the equation of state tables at the low-density edge. To make these corrections and extensions, we used a perfect-gas-radiation equation of state, adding analytic electrostatic corrections as described by Cox and Giuli (1968, chap. 15). We note that the results presented below are not at all sensitive to any inconsistencies in the envelope equation of state in this regime; the mass of envelope material involved is always less than $10^{-8} M_{\odot}$. The mass in the surface convection zone was always less than $10^{-10} M_{\odot}$.

The switch from the chemically inhomogeneous PNN models (which contain a small fraction of elements in addition to carbon, including a thin helium-rich surface layer) to the pure carbon PWD models necessitated some thermal relaxation to compensate for the slight change in the equation of state and opacities. At the epoch of the change in equation of state, the thermal time scale of the envelope (or, rather, of the surface helium layer of mass ΔM),

$$\tau \approx \int_{M_r}^{M_*} (c_v T/L) dm \sim (\bar{c}_v \bar{T} \Delta M)/L \quad (1)$$

(where L is the photon luminosity) is on the order of the evolution time scale (~ 1500 yr) through the rapid contraction phase. Therefore, relaxation to the new equation of state was accomplished by the time the sequence reached the PWD cooling track.

The evolutionary tracks in the H-R diagram are shown in Figure 1. Ages shown in Figure 1 are arbitrarily normalized to an age of 3000 yr when $\log(L/L_{\odot}) = 3.0$ for all sequences. From $\log(L/L_{\odot}) = 3.0$ to $\log(L/L_{\odot}) \sim 2.3$, the $0.60 M_{\odot}$ model evolves at roughly the same rate as comparable models of PNNs with nuclear burning (Iben 1984). But below $\log(L/L_{\odot}) \sim 2.3$, the current model evolved somewhat more slowly than those of Iben (1984) and Schönberner (1983) as composition and equation of state differences became important. Also in Figure 1 we have indicated (*solid bar*) the probable effective temperature limits for PG 1159-035. If that star is truly representative of the class, then those limits, along with $7 < \log g < 8$ imply that, for our models, luminosities between

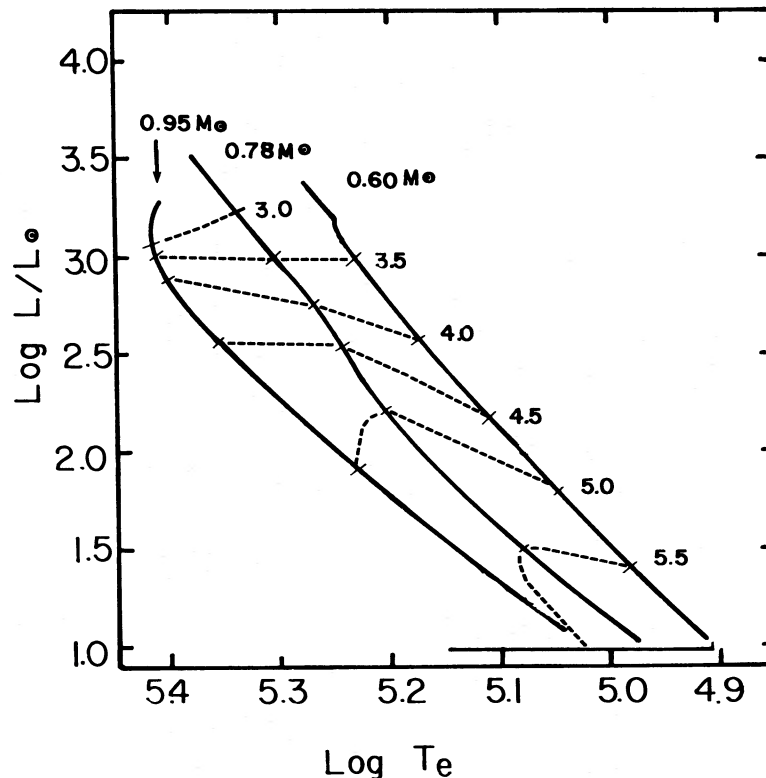


FIG. 1.—Evolutionary tracks of the 0.60 , 0.78 , and $0.95 M_{\odot}$ PWD evolutionary sequences from which equilibrium models were selected for pulsation analysis. Lines of constant age are indicated by dashed lines; these are labeled by the logarithm of the age in years. The ages indicated are normalized to $t = 3000$ yr at $\log(L/L_{\odot}) = 3.00$. The solid bar indicates the probable effective temperature limits for PG 1159-035.

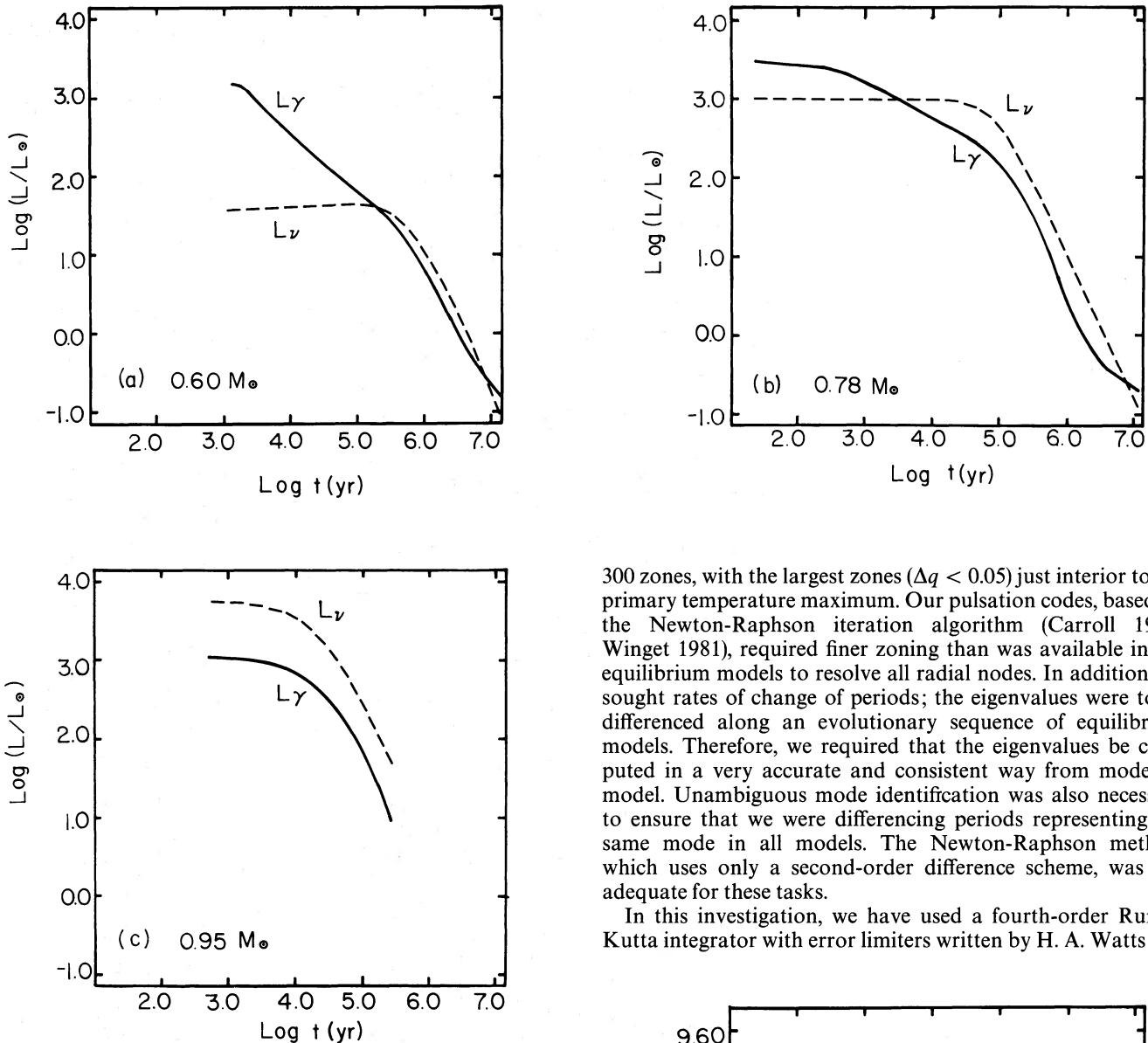


FIG. 2.—Luminosity as a function of time for (a) $0.60 M_{\odot}$, (b) $0.78 M_{\odot}$, and (c) $0.95 M_{\odot}$ PWD sequences. The solid line represents the photon luminosity; the total energy loss by neutrino emission is indicated by the dashed line.

$1 < \log(L/L_{\odot}) < 3$ are of interest. The luminosities (photon and neutrino) and radii as functions of time are shown in Figures 2 and 3. Note that for the 0.78 and $0.95 M_{\odot}$ sequences the neutrino luminosities dominate for all photon luminosities of interest.

III. PULSATION ANALYSIS

The nonradial oscillations of our PWD models were studied using a computer code which solves the equations of linear, nonradial adiabatic oscillations as formulated by Dziembowski (1971). As Starrfield *et al.* (1983, 1984) demonstrated, if the observed pulsations in the pulsating PG 1159 stars are indeed nonradial gravity modes, then they must be very high order overtones, which means many nodes in the displacement eigenfunction. The input models contained between 250 and

300 zones, with the largest zones ($\Delta q < 0.05$) just interior to the primary temperature maximum. Our pulsation codes, based on the Newton-Raphson iteration algorithm (Carroll 1981; Winget 1981), required finer zoning than was available in the equilibrium models to resolve all radial nodes. In addition, we sought rates of change of periods; the eigenvalues were to be differenced along an evolutionary sequence of equilibrium models. Therefore, we required that the eigenvalues be computed in a very accurate and consistent way from model to model. Unambiguous mode identification was also necessary to ensure that we were differencing periods representing the same mode in all models. The Newton-Raphson method, which uses only a second-order difference scheme, was not adequate for these tasks.

In this investigation, we have used a fourth-order Runge-Kutta integrator with error limiters written by H. A. Watts and

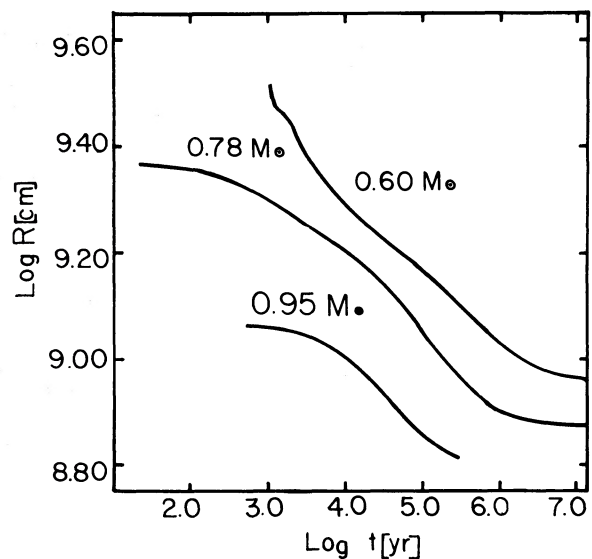


FIG. 3.—Radius as a function of time for the three PWD sequences: (top) $0.60 M_{\odot}$, (middle) $0.78 M_{\odot}$, and (bottom) $0.95 M_{\odot}$.

L. F. Shampine of Sandia Laboratories. The overall method of solving the eigenvalue problem is by "shooting" from the model center to its surface in an iterative fashion until all boundary conditions are satisfied. To resolve closely spaced nodes, the equilibrium model quantities are interpolated between zones, by means of cubic splines, in the process of integration. This typically results in 2000–3000 effective zones. This procedure produces periods and eigenfunctions that are insensitive to the zoning details of the equilibrium models. The phase-diagram scheme (Scuflaire 1974; Osaki 1975; see also Unno *et al.* 1979, § 16, or Cox 1980, § 17.11) of mode classification has been used to evaluate the order of, and hence identify, a given mode. For white dwarfs, which are relatively simple beasts, this scheme was straightforward to apply. We neither missed nor misidentified a mode as it evolved in time.

For simplicity in this study, we have considered only dipole ($l = 1$) and quadrupole ($l = 2$) modes. The amplitude of the observed pulsations in the PG 1159 stars is relatively high ($\sim 1\%$). For a given perturbation displacement, geometric cancellation effects greatly reduce the resultant luminosity variation (averaged over the visible hemisphere) for $l \geq 3$ (Dziembowski 1977). Therefore, low l -modes are most likely responsible for the observed variation of the pulsating PG 1159 stars.

We want to understand which physical properties of PWDs most strongly affect their pulsation properties. To interpret the numerical results, we relied on two pulsation diagnostics: propagation diagrams and weight functions. Propagation diagrams, as discussed below, are useful predictors of the global properties of nonradial oscillations and are based on model structure. We also describe nonradial weight functions, which provide us with a way to identify regions within a model that contribute to setting the pulsation period.

a) Propagation Diagrams

The global trends in the properties of nonradial oscillations are well illustrated with the use of propagation diagrams. These plots of the squares of the Brunt-Väisälä frequency (N^2) and the acoustic frequency (S_l^2) as functions of position within a stellar model graphically illustrate the regions of a model within which a nonradial mode may propagate. (For a complete discussion see Unno *et al.* 1979, § 14; Cox 1980, § 17.10.)

Although the full set of adiabatic equations was used in the calculations, in the following analytical discussion we neglect perturbations in the gravitational potential (the Cowling approximation). This is a reasonable assumption for the high-order modes which are mainly of interest here. We assume that the radial part of the eigenfunction is proportional to e^{ikr} , where k is the radial wavenumber. In this limit, the adiabatic equations lead to a local dispersion relation for the radial wavenumber k :

$$k^2 = (\sigma^2 c_s^2)^{-1} (\sigma^2 - S_l^2) (\sigma^2 - N^2), \quad (2)$$

where

$$N^2 = -gA, \quad (3)$$

$$A \equiv \frac{1}{\rho} \frac{d\rho}{dr} - \frac{1}{\Gamma_1 P} \frac{dP}{dr}, \quad (4)$$

and

$$S_l^2 \equiv \frac{l(l+1)\Gamma_1 P}{r^2 \rho} = l(l+1) \frac{c_s^2}{r^2}. \quad (5)$$

Here σ is the eigenfrequency, c_s is the local adiabatic sound speed, P is the total pressure, and l is the colatitudinal angular index in the spherical harmonic $Y_l^m(\Theta, \Phi)$; other symbols have their usual meanings. Clearly A is related to the Schwarzschild criterion for convective stability, so that N^2 is rendered negative in regions of convective instability.

The dispersion relation (2) shows under what conditions a given mode is locally propagating. If σ^2 is either greater than both S_l^2 and N^2 (pressure modes) or less than both of those frequencies (g -modes), then $k^2 > 0$ and the mode is oscillatory and propagates locally. Otherwise $k^2 < 0$, and the mode is locally evanescent.

Thus, the nonradial g -mode propagation zone is represented by the condition $\sigma^2 < S_l^2, N^2$. In Figure 4 we show a typical propagation diagram for an early PWD model with a convection zone near the surface. In a centrally condensed model, there may exist a local maximum in N^2 at the point in the star below which most of the mass is contained (Cox 1980, § 17.10). In this model, with central condensation ($\rho_c/\bar{\rho}$) of 49.7, that point is at $r/R_* \sim 0.4$. We expect, then, that low-order (high-frequency) g -modes may be effectively trapped below that point.

As the PWD evolves, the central condensation decreases, and the degeneracy boundary moves outward in mass. Since degeneracy results in neutral stratification (Osaki and Hansen 1973), N^2 will decrease, and the local maximum will decrease in contrast. Hence, the expectation is that, as evolution proceeds, the periods of the nonradial g -modes should generally increase and the region of propagation should gradually shift toward the outer portions of the star.

b) Variational Principle

The equations of motion for adiabatic nonradial oscillations may be derived from a variational principle which expresses the frequency eigenvalue in terms of total integrals of the eigenfunctions weighted by various physical quantities taken from

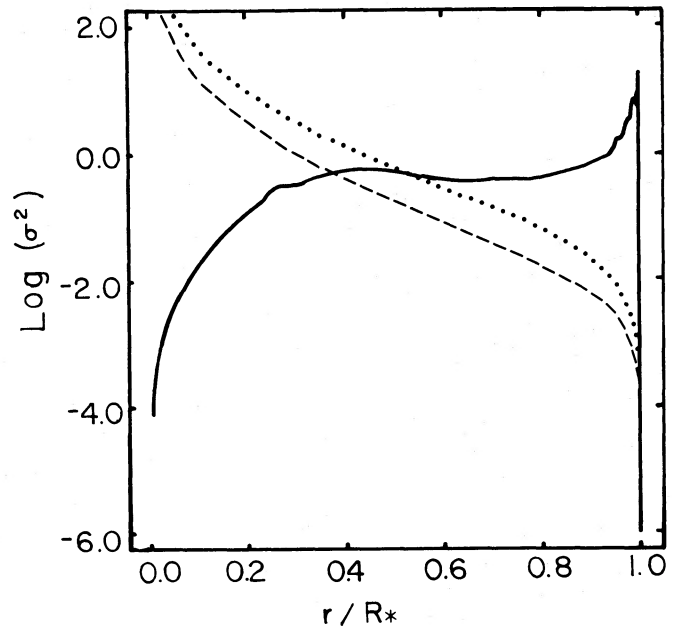


FIG. 4.—Propagation diagram for $0.95 M_{\odot}$ at $\log(L/L_{\odot}) = 3.10$. The solid line is the square of the Brunt-Väisälä frequency (N^2). The dashed line is the square of the acoustic frequency (S_l^2) for $l = 1$; the dotted line, for $S_l^2, l = 2$.

the evolutionary equilibrium stellar model. In the usual formulation it is assumed that both the pressure and the density vanish at the stellar surface ("zero" boundary conditions). This assumption, coupled with the self-adjoint nature of the adiabatic system, is sufficient to demonstrate the variational properties.

As we will show, the variational expression for σ^2 may be cast in the form

$$\sigma^2 = \frac{\int f(Y(x), x) dx}{\int g(Y(x), x) dx}, \quad (6)$$

where x is some stellar quantity such as radius, $Y(x)$ is a quadratic function of the eigenfunctions, y (as in Dziembowski 1971), and $f(y, x)$ and $g(y, x)$ are functionals of the indicated arguments. The denominator is proportional to the kinetic energy of oscillation. The integrand of the numerator serves as a "weight" function, in that its relative values through the star inform us, in effect, where the eigenvalue is established. It has been used in an astrophysical context by Epstein (1950), Goossens and Smeyers (1974), and Schwank (1976), among others. The formulation we shall use is based on that of Unno *et al.* (1979, § 13). After performing some integrations by parts, we may combine equations (13.13) and (13.15) of Unno *et al.* and the definitions of the Dziembowski variables y , to find

$$\sigma^2 = \frac{\int_0^R [C(y, r) + N(y, r) + G(y, r)] \rho r^2 dr}{\int_0^R T(y, r) \rho r^2 dr}, \quad (7)$$

where

$$T(y, r) = r^2 \left[y_1^2 + l(l+1) \left(\frac{g}{r\sigma^2} \right)^2 y_2^2 \right], \quad (8a)$$

$$C(y, r) = g^2 l(l+1) S_l^{-2} (y_2 - y_3)^2, \quad (8b)$$

$$N(y, r) = r^2 N^2 y_1^2, \quad (8c)$$

$$G(y, r) = -\frac{gr}{U} [y_4 + l(l+1)y_3]^2. \quad (8d)$$

Here $T(y, r)$ is proportional to the kinetic energy density, $C(y, r)$ contains the square of the acoustic frequency, $N(y, r)$ varies directly with the Brunt-Väisälä frequency $N^2(r)$, and the perturbative information in $G(y, r)$ involves only the gravitational eigenfunctions y_3 and y_4 . Thus, C , N , and G may be regarded as weight functions which individually provide diagnostic information on acoustic, gravity wave, and gravitational field contributions to σ^2 . For example, if $N^2(r)$ were to change by a small amount δN^2 without any corresponding change in the other physical characteristics of the static model (which is highly unlikely), then it may easily be shown that the eigenvalue would change by

$$\delta\sigma^2 = \frac{\int_0^R N(y, r) (\delta N^2 / N^2) \rho r^2 dr}{T(R)}. \quad (9)$$

(Note that Rayleigh's principle guarantees that induced changes in the eigenfunctions need not be considered because those changes would result in second-order corrections to σ^2 .) $N(y, r)$ is then a kernel for $\delta\sigma^2 / \delta N^2$. Such kernels are an essential ingredient in stellar seismic diagnostics and inverse theory and are presently being explored for solar (Deubner and Gough 1984) and terrestrial (Backus and Gilbert 1967) seismology. In this work we shall use these kernels to guide us in

our interpretation of the oscillation behavior of hot PWD stars.

Another use of the variational principle is as a numerical check on the accuracy of the computed eigenfunctions. That is, computed eigenfunctions are inserted in equations (6) and (7) to find the variational value of σ^2 . This is then compared with that value computed directly from the analysis that yielded the eigenfunctions in the first place. The agreement between the variational value of σ^2 and the directly computed value may be considered a figure of merit for σ^2 . We find agreement to 3–5 significant figures in σ^2 computed in these two ways. Some of this small error is most certainly attributable to differences in the surface boundary condition employed by the two techniques. The variational expressions given here require the vanishing of surface pressure and density, whereas we employ somewhat more realistic subsurface boundary conditions for the Runge-Kutta integrations (Winget 1981).

IV. RESULTS

a) Weight Functions

The transition from the centrally condensed planetary nebula nucleus to the white dwarf configuration is accompanied by a striking change in the character of the weight function (the integrand of the numerator of eq. [6]). There is a narrow transition range in luminosity where the maximum of the weight function for high-order modes moves from well inside the degenerate core [$q \equiv m_*/M_* \sim 0.50$] out to the outer envelope ($q \sim 0.98$). This is illustrated in Figure 5 for a $g_{25}, l = 1$ mode (period of ~ 550 – 650 s) followed through the evolution of our $0.60 M_\odot$ model.

At high luminosities the $g_{25}, l = 1$ mode was uniformly weighted through most of the degenerate interior. Figure 5a is comparable to Figure 1 of Schwank (1976) for the $g_3, l = 2$ mode of an $n = 3$ polytrope (intermediate central condensation). As the star cooled, the weight of the surface increased relative to the interior as was anticipated from our previous discussion. After the model dropped below a transition luminosity of $\log(L/L_\odot) = 2.0$ for this $0.60 M_\odot$ sequence, the surface weight dominated. The degeneracy boundary of the hot models was at $q \sim 0.85$ (which moved slowly outward with time), so that at high-luminosity phases the adiabatic properties of the pulsations should have reflected the conditions in the degenerate core. After the transition from the more global contributions to envelope dominance of the weight function, the mode became increasingly affected by the conditions between the edge of the degenerate core and the surface.

The oscillatory behavior of the weight functions in Figure 5 reflects their dependence on the eigenfunctions. The overwhelming contribution to the weight is from the gravity-wave term $N(r)$, as should be expected for a g -mode. At low luminosities the compressional term $[C(r)]$ also contributes to the weight in the envelope. The transition of the maximum in the weight function from core to surface reflects the decrease in central condensation as well as evolutionary changes at fixed mass points (Schwank 1976).

The running integral of the weight function, from stellar center to a given fractional radius, is shown as a function of that fractional radius in Figure 6. Such "leaf diagrams" show that, through the high-luminosity phases, the period is determined primarily in the degenerate interior within $q < 0.9$, and that the distribution of weight with mass is approximately con-

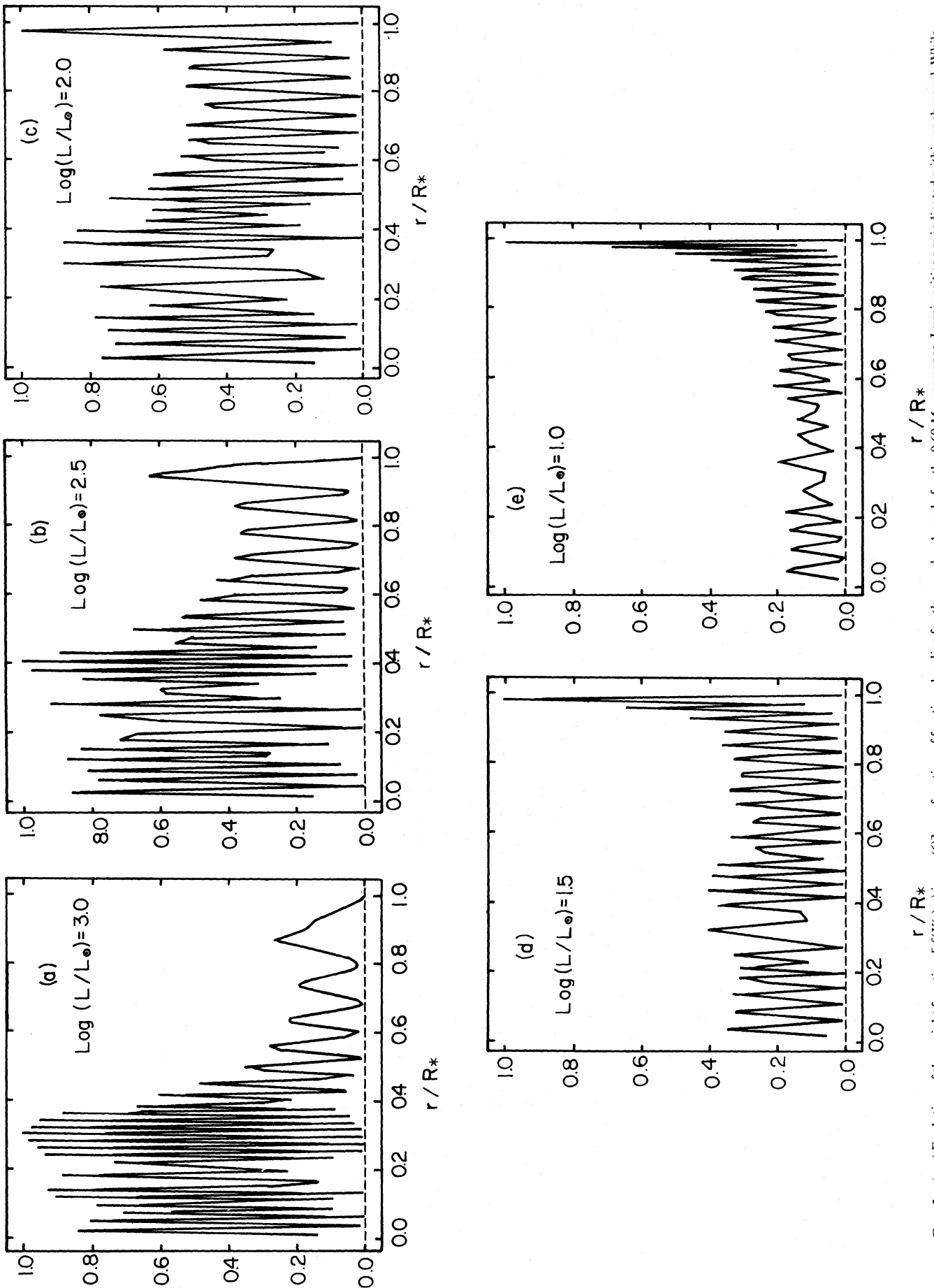


FIG. 5.—(a-e) Evolution of the weight function $[f(Y(r), r)]$ as a function of fractional radius for the $0.60 M_{\odot}$ sequence. Luminosities are indicated within each panel. While the weight functions were originally computed using finer zoning (see § III), the value of the weight function is plotted for the mass zoning of the input model; hence, near $r/R_{*} = 0.2-0.4$ the curve is underresolved.

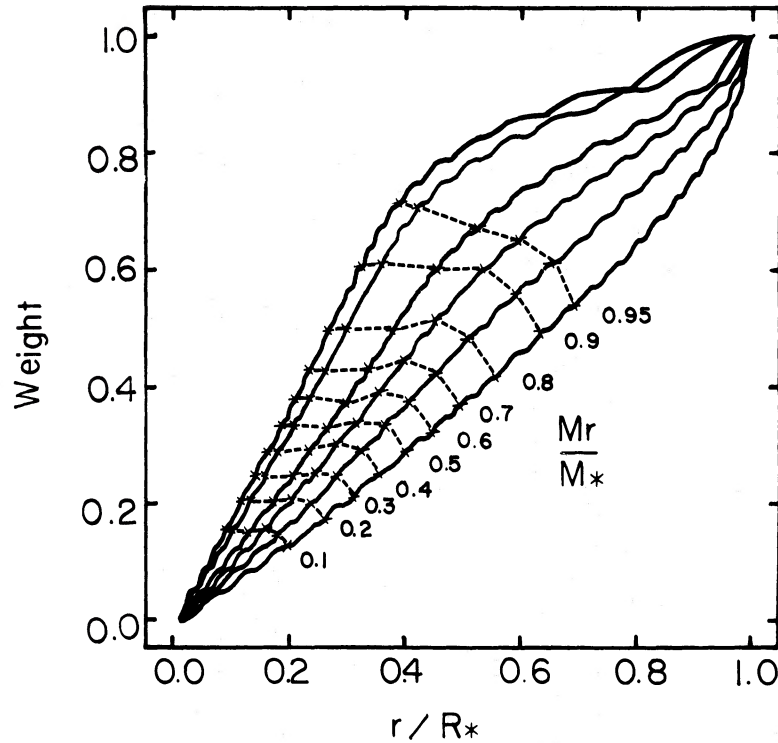


FIG. 6.—Running integral of the weight functions (see Fig. 5) to a given fractional radius for the g_{25} , $l = 1$ mode in the $0.60 M_{\odot}$ sequence. From top to bottom, lines are $\log(L/L_{\odot}) = 3.15, 3.00, 2.50, 2.00, 1.50,$ and 1.00 . The mass fraction is indicated along the curves.

stant there. At these luminosities, the pulsation properties retain some similarities to those of the red giants of which these models are descendants (Schwank 1976). Below the transition luminosity the surface has become important; the integrated weight remains low in the core and increases quickly with radius near the surface. The pulsations have become white dwarf-like in character.

We find that the behavior of the weights as functions of time and position in an evolutionary sequence is approximately the same for all g -modes with $k > 10$ and $l = 1, 2$.

b) Eigenfunctions, Periods, and dP/dt

The periods of some high-order modes for the three evolutionary sequences are presented in Tables 1–3. Periods of the range seen in the pulsating PG 1159 stars correspond to roughly $k = 25$ (for the $0.60 M_{\odot}$ models) to $k = 51$ (for the $0.95 M_{\odot}$ models) for $l = 1$. For high-order g -modes the period for a given k scales as the square root of $[l(l+1)]^{-1}$ (see Cox 1980, § 17.12); to obtain periods of ~ 550 s for $l = 2$, the order of a mode would have to increase by a factor of ~ 1.7 .

In Figure 7 we show representative radial ($\delta r/r$) and horizontal ($\delta t/r$) displacements for $k = 25$, $l = 1$ in two $0.60 M_{\odot}$ models. These have been normalized to $\delta r/r = 1$ at $r = R_*$. As we see, the motion is dominated by the tangential component of the displacement in the outer stellar regions. In the high-luminosity models with high central condensation the maximum amplitude of the total displacement near the center is about 1/30 of the displacement at the surface. As the star cooled, the relative amplitude of surface displacement grew and the tangential displacement grew relative to the radial displacement.

Also included in Tables 1–3 are the rates of change of the periods with time (dP/dt). These values of dP/dt were derived

by differencing the calculated periods for consecutive evolutionary models ($\Delta \log [t(\text{yr})] < 0.1$) and dividing by the age difference of the equilibrium models. Presumably, the modes of pulsation of the PG 1159 stars are self-exciting; hence non-adiabatic contributions to the period may be significant when dP/dt is being calculated. These, too, will change time time as the star evolves through the instability strip. The adiabatic value of dP/dt , then, should be considered an estimate of the magnitude of the overall value of dP/dt .

We find the adiabatic periods of the high-order modes to be increasing (positive dP/dt) in all models below $\log(L/L_{\odot}) = 2.5$. When the luminosity of the model is above the transition luminosity (see previous section), the time scale for period change $[(d \ln P/dt)^{-1}]$ is long compared with e -folding times for surface variables such as luminosity and effective temperature. As we will now show, this reflects the fact that the period is being established throughout the interior of the model, where the cooling and contraction time scales correspond to the thermal time scale of the whole star, $\sim 10^6$ yr.

WHVH have proposed, on physical grounds, that the expression for dP/dt should have the form

$$\frac{1}{P} \frac{dP}{dt} = -\frac{a}{T} \frac{dT}{dt} + \frac{b}{R} \frac{dR}{dt}, \quad (10)$$

where T is the temperature in the region of maximum weight and R is the stellar radius. Cooling effects tend to increase the periods of high-order g -modes (because of decreasing N^2), while contraction effects lead to decreasing periods, with the resulting general increase in sound speed (see § IIIa). The factors a and b in equation (10) are of order unity and are affected by properties such as the temperature dependence of the specific heats, the amount of mass contributing to setting

TABLE 1
PULSATION PROPERTIES OF 0.60 M_{\odot} PWD MODELS

AGE (yr)	$\log(L/L_{\odot})$	g_1			g_{10}			g_{25}			g_{35}		
		Period (s)	dP/dt ($s\ s^{-1}$)	Period (s)	dP/dt ($s\ s^{-1}$)	Period (s)	dP/dt ($s\ s^{-1}$)	Period (s)	dP/dt ($s\ s^{-1}$)	Period (s)	dP/dt ($s\ s^{-1}$)	Period (s)	dP/dt ($s\ s^{-1}$)
1.909(+3)	3.150	55.310	-2.70(-11)	243.870	1.34(-11)	559.042	-6.42(-11)	767.028	-1.04(-10)	448.050	-4.64(-11)		
2.424(+3)	3.081	54.925	-2.08(-11)	244.291	3.35(-11)	558.766	2.62(-12)	766.269	-2.29(-11)	447.533	-1.71(-11)		
2.985(+3)	3.002	54.615	-1.50(-11)	245.038	4.31(-11)	559.210	3.14(-11)	766.346	6.47(-12)	447.526	1.44(-12)		
4.267(+3)	2.856	54.166	-8.15(-12)	246.659	3.53(-11)	560.890	4.53(-11)	766.765	1.96(-11)	447.722	1.16(-11)		
6.385(+3)	2.705	53.811	-3.60(-12)	248.455	2.13(-11)	563.545	3.19(-11)	768.713	2.98(-11)	448.969	1.82(-11)		
1.142(+4)	2.500	53.509	-9.13(-13)	250.958	1.25(-11)	566.687	1.37(-11)	773.585	2.27(-11)	451.755	1.29(-11)		
2.191(+4)	2.273	53.467	2.54(-13)	253.991	7.26(-12)	570.594	9.89(-12)	778.182	1.21(-11)	454.330	6.93(-12)		
5.313(+4)	2.000	53.988	6.12(-13)	258.999	4.04(-12)	577.268	5.85(-12)	788.073	8.23(-12)	460.170	4.85(-12)		
1.065(+5)	1.776	55.059	6.34(-13)	264.246	2.49(-12)	584.741	3.45(-12)	799.446	5.68(-12)	466.837	3.32(-12)		
2.507(+5)	1.500	57.913	6.27(-13)	272.185	1.48(-12)	596.313	2.96(-12)	819.282	4.20(-12)	478.377	2.47(-12)		
4.126(+5)	1.304	61.143	6.06(-13)	278.778	1.30(-12)	613.048	3.25(-12)	840.275	4.21(-12)	490.818	2.48(-12)		
7.429(+5)	1.000	66.954	5.05(-13)	292.889	1.31(-12)	646.179	2.95(-12)	886.222	3.93(-12)	517.714	2.30(-12)		

NOTE.—Numbers in parentheses: 1.909(+3) = 1.909 $\times 10^3$.

TABLE 2
PULSATION PROPERTIES OF $0.78 M_{\odot}$ PWD MODELS

AGE (yr)	$\log(L/L_{\odot})$	$l = 1$						$l = 2$	
		g_1		g_{10}		g_{35}		g_{39}	
		Period (s)	dP/dt ($s s^{-1}$)	Period (s)	dP/dt ($s s^{-1}$)	Period (s)	dP/dt ($s s^{-1}$)	Period (s)	dP/dt ($s s^{-1}$)
1.746(+3).....	3.115	38.230	-5.68(-12)	174.456	3.42(-11)	544.556	5.35(-11)
3.000(+3).....	3.000	38.038	-4.23(-12)	175.490	2.03(-11)	545.864	2.22(-11)	352.171	1.46(-11)
5.934(+3).....	2.853	37.719	-2.81(-12)	176.729	9.11(-12)	546.850	5.61(-12)	352.864	3.49(-12)
7.064(+3).....	2.817	37.625	-2.53(-12)	177.035	7.78(-12)	547.035	4.68(-12)	352.975	2.85(-12)
1.210(+4).....	2.707	37.276	-1.85(-12)	177.870	2.25(-12)	547.109	-2.90(-12)	353.301	9.42(-14)
1.779(+4).....	2.631	37.007	-1.18(-12)	178.051	9.47(-13)	546.299	-4.24(-12)	353.114	-1.80(-12)
3.249(+4).....	2.516	36.657	-3.19(-13)	178.383	4.91(-13)	544.907	-8.38(-13)	351.940	-1.72(-12)
4.333(+4).....	2.454	36.602	6.27(-14)	178.729	1.16(-12)	544.820	4.45(-13)	351.634	3.67(-13)
8.623(+4).....	2.252	37.450	8.69(-13)	181.527	2.83(-12)	550.399	6.62(-12)	356.316	4.76(-12)
1.501(+5).....	1.999	39.621	1.24(-12)	188.921	4.16(-12)	568.625	1.05(-11)	368.067	6.52(-12)
2.127(+5).....	1.787	42.489	1.42(-12)	197.298	3.85(-12)	590.168	1.06(-11)	381.586	6.80(-12)
3.181(+5).....	1.499	47.080	1.32(-12)	208.226	3.09(-12)	624.013	9.80(-12)	404.119	6.36(-12)
5.623(+5).....	1.015	56.488	1.10(-12)	230.857	2.69(-12)	693.908	8.00(-12)

NOTE.—Numbers in parentheses: $1.746(+3) = 1.746 \times 10^3$.

the period, the importance of local neutrino energy losses, and other effects such as rotation and nonadiabaticity. The relevant evolutionary time scale, therefore, gives an upper limit to the rate of period change.

We can define a parameter, s , as the ratio of the contraction rate to the cooling rate:

$$s \frac{d \ln T}{dt} = \frac{d \ln R}{dt} \quad (11)$$

Using this ratio, we can rewrite equation (10) as

$$\frac{\dot{P}}{P} = (-a + bs) \frac{\dot{T}}{T} \quad (12)$$

At high luminosities, where contraction dominates ($s > 1$), the rate of period decrease is approximated by the rate of radius decrease. When cooling dominates ($s < 1$), then the rate of period increase is of the same order as the cooling rate. When the competing effects of cooling and contraction are in approximate balance ($s \sim 1$), then the magnitude of dP/dt can be very small or zero, corresponding to a long time scale for period change. The luminosity where this occurs in a given model depends on the combination of factors (all of order unity) in equation (11) and is accompanied by a sign change in dP/dt .

At very high luminosities [$\log(L/L_{\odot}) > 3.0$] in the 0.95 and $0.60 M_{\odot}$ models, global contraction effects dominate. Time scales for radius decrease in these models are much shorter than cooling time scales in the zone of large weight. The

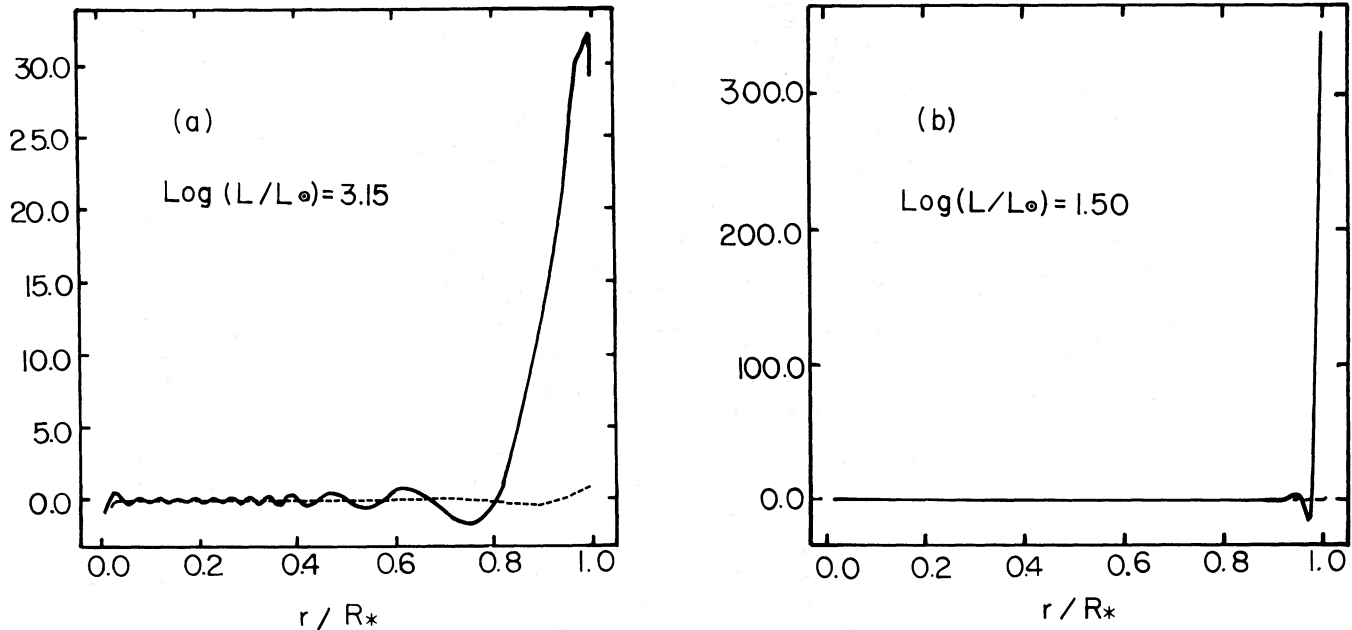


FIG. 7.—Radial (dashed line) and horizontal (solid line) displacement perturbations for the g_{25} , $l = 1$ mode, normalized to the radial displacement at the surface, for (a) $\log(L/L_{\odot}) = 3.15$ and (b) $\log(L/L_{\odot}) = 1.50$.

TABLE 3
PULSATION PROPERTIES 0.95 M_{\odot} PWD MODELS

AGE (yr)	$\log(L/L_{\odot})$	$l = 1$						$l = 2$					
		g_1		g_{10}		g_{35}		g_{51}		g_{35}		g_{51}	
		Period (s)	dP/dt ($s s^{-1}$)	Period (s)	dP/dt ($s s^{-1}$)	Period (s)	dP/dt ($s s^{-1}$)	Period (s)	dP/dt ($s s^{-1}$)	Period (s)	dP/dt ($s s^{-1}$)	Period (s)	dP/dt ($s s^{-1}$)
-5.470(+3).....	3.152	25.389	-3.75(-12)	124.677	-1.32(-11)	385.000	-4.66(-11)	548.062	-7.40(-11)	225.144	-2.77(-11)		
-2.170(+3).....	3.095	25.076	-2.27(-12)	123.625	-7.03(-12)	381.010	-3.01(-11)	541.944	-4.36(-11)	222.771	-1.79(-11)		
3.380(+3).....	2.993	24.903	-1.12(-13)	123.346	7.49(-13)	378.255	-7.43(-12)	538.948	-5.36(-12)	221.151	-4.35(-12)		
1.675(+4).....	2.762	25.704	2.36(-12)	125.926	6.55(-12)	383.024	1.39(-11)	547.942	2.39(-11)	223.988	8.22(-12)		
3.926(+4).....	2.454	27.877	3.06(-12)	131.042	8.21(-12)	395.562	2.14(-11)	567.515	3.08(-11)	231.331	1.25(-11)		
5.706(+4).....	2.261	29.604	3.30(-12)	136.056	9.07(-12)	409.000	2.47(-11)	586.060	3.47(-11)	239.208	1.45(-11)		
7.136(+4).....	2.128	31.179	3.37(-12)	140.206	8.84(-12)	420.416	2.44(-11)	602.266	3.49(-11)	245.959	1.44(-11)		
1.186(+5).....	1.776	35.689	2.85(-12)	151.925	6.89(-12)	453.385	2.01(-11)	649.936	2.91(-11)	265.121	1.18(-11)		
1.729(+5).....	1.478	40.289	2.44(-12)	162.206	5.65(-12)	484.738	1.69(-11)	695.433	2.47(-11)	283.592	9.93(-12)		
2.279(+5).....	1.237	44.118	2.10(-12)	171.523	5.03(-12)	512.075	1.49(-11)	735.630	2.17(-11)	299.549	8.69(-12)		
3.005(+5).....	0.981	543.886	1.26(-11)	318.207	7.42(-12)		

NOTE.—Numbers in parentheses: -5.470(+3) = -5.470 × 10³.

decreasing periods of these models reflect this condition. Following this phase of rapid contraction, the further radius changes are tempered by the stiffening of the equation of state, and these models approach the constant-radius phase of evolution. At this time, periods start to increase with time. The behavior of $d \ln P/dt$ as a function of luminosity is presented in Figure 8 for the $g_{35}, l = 1$ mode in the three sequences.

There was a range in luminosities in the $0.78 M_{\odot}$ model that yielded negative values for dP/dt . This phase occurred just prior to the broad kink in the evolutionary track for this model (see Fig. 1). This effect is related to the diffusion of residual thermal energy from the fossil-burning shell. The burning shell imposed the steep temperature gradient near the surface, providing radiative support for the overlying mass. As the excess thermal energy diffused into regions with a very short thermal time scale, this excess support dissipated. The radius of the regions of the star below the temperature excess then decreased as the new, shallower temperature gradient became established. If the zone of excess thermal energy moves through a region of the star important in setting the oscillation frequency, a negative dP/dt could result from the *local* radius adjustment.

We can make use of the delay between the onset of negative dP/dt and the completion of the kink in the evolutionary track to estimate the depth at which the pulsation period is determined. From Figure 3 we see that the stellar radius began to decrease more rapidly at an age of about 4×10^4 yr. Negative dP/dt appeared at an age of about 7×10^3 yr. The difference in time should be comparable to the thermal time scale (defined in eq. [1]) of the region where the period was determined in the model. Using these values, we find that the delay corresponds to a depth of $0.08 M_{\odot}$ below the surface, implying that the period was determined around the position of the degeneracy boundary. This is in qualitative agreement with the weight function for $0.78 M_{\odot}$ models at a value of $\log(L/L_{\odot})$ of about 2.6.

More careful treatment of the cessation of nuclear burning in the PWD phase may alter the timetable of outward diffusion of thermal energy of the burning shell. The transformation from a temperature profile for nuclear burning to one of gravitational contraction will be more gradual than in the simple models presented in this paper. Hence any of the readjustments in radius such as those that produced negative values of dP/dt would be less abrupt in more realistic models.

The detailed behavior of dP/dt as a function of time was not well determined for those high-luminosity, rapidly evolving models where the difference between periods in successive models was comparable to our estimates of possible period errors, as in § IIIb. Hence, error bars of approximately $\pm 1 \times 10^{-14}$ should properly be attached to $d \ln P/dt$ above $\log(L/L_{\odot}) \sim 2.75$ for the 0.60 and $0.95 M_{\odot}$ sequences in Figure 8. Also, above $\log(L/L_{\odot}) = 2.6$ for the $0.78 M_{\odot}$ sequence, the period difference between consecutive models was quite small (< 0.2 s).

At luminosities below $\log(L/L_{\odot}) = 2.5$, all models showed increasing periods. For these models, dP/dt was far more reliable than for those at higher luminosities; period changes between successive models were much greater than the expected internal errors. The time scales for period change [$\tau = (d \ln P/dt)^{-1}$] ranged from 8×10^5 to 20×10^5 yr at these lower luminosities. The time scale varies inversely with mass at a given luminosity for a given mode.

In § IIIa the relationship of the time dependence of the oscillation period to the evolutionary changes in the Brunt-Väisälä frequency was discussed with reference to propagation diagrams. This relationship is illustrated in Figure 9. The $g_{35}, l = 1$ mode for the $0.95 M_{\odot}$ model has $dP/dt = -5 \times 10^{-11}$ in Figure 9a and $dP/dt = +2 \times 10^{-11}$ in Figure 9b. The integrated weight function for this mode is indicated with arrows above the N^2 curves in Figure 9. Note that the bulk of the eigenvalue is determined before the zone of increasing N^2 in Figure 9b.

V. CONCLUSIONS

In cooling from a hot, centrally condensed state to a white dwarf configuration, the nonradial pulsation properties of hot PWDs go through a distinct transformation. At high luminosities, their g -mode oscillation characteristics are somewhat reminiscent of those of red giants and other centrally condensed stars (Schwank 1976; Unno *et al.* 1979). At this stage, eigenfunctions of the spatial perturbations of hot PWDs have some amplitude throughout the star, and the period is largely determined in the degenerate core. Upon cooling below a critical luminosity, the oscillation characteristics transform to those expected for the white dwarf stars (Osaki and Hansen 1973; Brickhill 1975; Winget and Fontaine 1982). For those, the perturbation displacements have largest amplitude near the

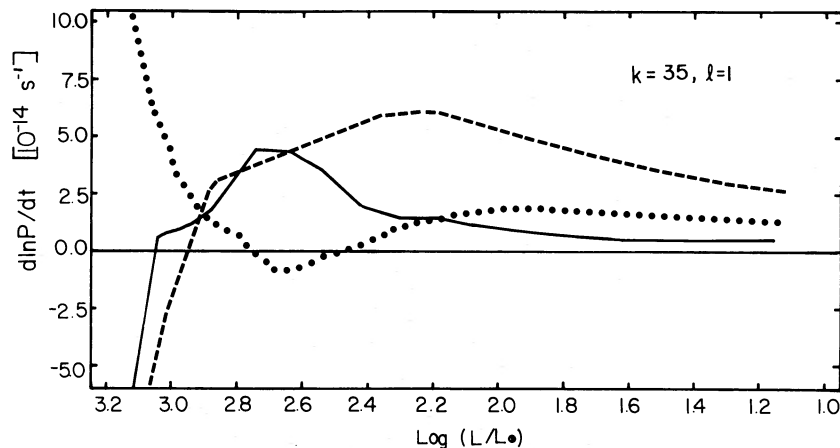


FIG. 8.—The relative rate of period change, $d \ln P/dt$ (s^{-1}), as a function of luminosity for the $g_{35}, l = 1$ mode in the $0.60 M_{\odot}$ (solid curve), $0.78 M_{\odot}$ (dotted curve), and the $0.95 M_{\odot}$ (dashed curve) sequences.

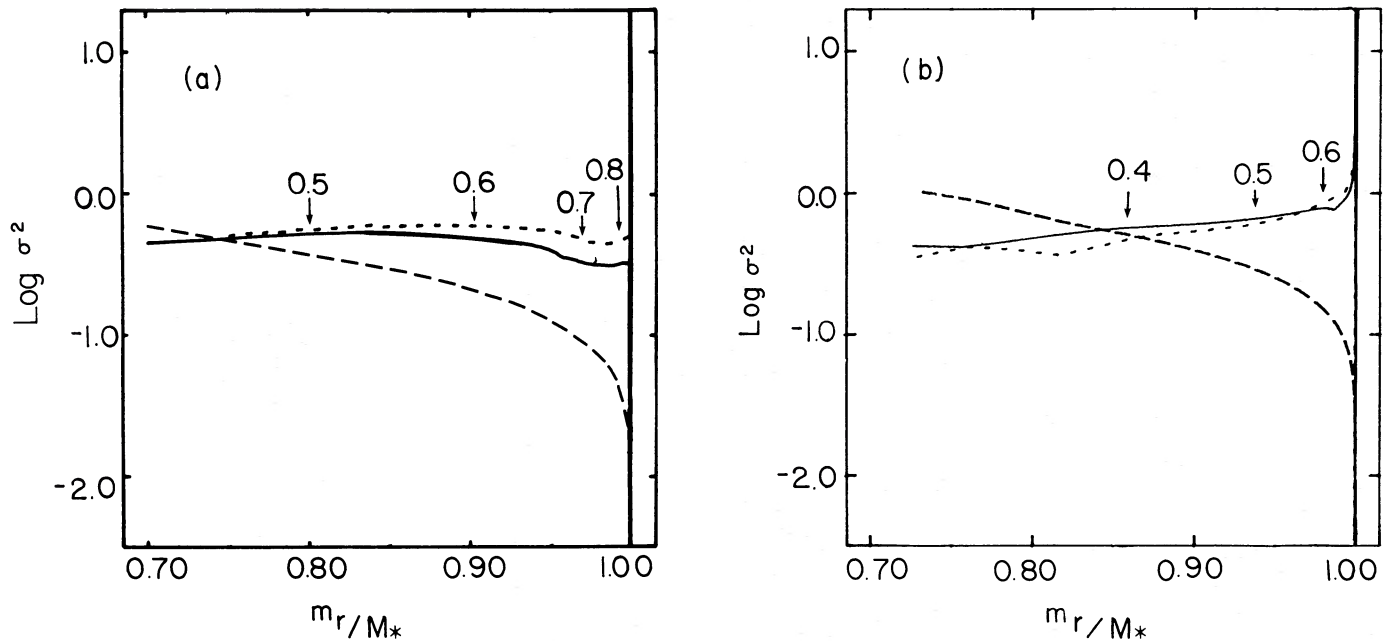


FIG. 9.—Expanded propagation diagrams for some $0.95 M_{\odot}$ models. (a) Solid line: N^2 for $\log(L/L_{\odot}) = 3.15$; short-dashed line: N^2 for $\log(L/L_{\odot}) = 3.10$. (b) Solid line: N^2 for $\log(L/L_{\odot}) = 2.45$; short-dashed line: N^2 for $\log(L/L_{\odot}) = 2.13$. The long-dashed line is S_l^2 for $l = 1$ in the more luminous model.

surface; the weight functions indicate that the outer few percent of the mass of the star contributes most to establishing the period of oscillation of the high-order g -modes.

High-order g -modes are required in all models to match the period observed in the pulsating PG 1159 stars. For $l = 1$, periods of about 500 s are given by values of $k > 20$ for the $0.60 M_{\odot}$ models and $k > 35$ for the $0.95 M_{\odot}$ models.

At luminosities of $\log(L/L_{\odot}) < 3.0$, periods generally increase with time. The time scale for period increase is comparable to the time scale for cooling in the region of maximum weight as a result of the temperature dependence of the local Brunt-Väisälä frequency. When the weight function is large in the stellar core, then the e -folding time for period increase is long compared to the time scale for, for example, change in effective temperature. After the model cools below the transition luminosity, with the weight function large near the surface, the time scale for period change is of the order of the e -folding time for the effective temperature.

At $\log(L/L_{\odot}) = 2.0$, corresponding to the middle of the estimated range of luminosity of the pulsating PG 1159 stars, the time scale for period increase for the PWD models ranged from 0.6×10^6 to 3×10^6 yr for masses of 0.95 and $0.60 M_{\odot}$, respectively. Time scales for surface temperature cooling were about $(0.3\text{--}0.7) \times 10^6$ yr for the same models. At $\log(L/L_{\odot}) = 2.0$, the 0.95 and $0.78 M_{\odot}$ models had cooled below their transition luminosities. The periods of these higher mass models were formed near the surface, where the representative cooling rate can be approximated by the change in effective temperature. Their cooling time scales were about half their period-change time scales, in agreement with the relation of WHVH and equation (12) when the temperature changes correspond to a cooling gas with nondegenerate electrons providing the heat capacity. The transition luminosity for the $0.60 M_{\odot}$ model is at about $\log(L/L_{\odot}) = 2.0$. Its time scale for period change was somewhat longer than the e -folding time scale of the surface temperature because the contribution of the core to setting the period was still important at this luminosity.

These conclusions appear to hold for the entire class of standard post-PNN models. Using evolutionary models from a $0.60 M_{\odot}$ sequence of post-PNN models of Iben (private communication), we found a time scale for period increase of 0.3×10^6 yr for the g_{20} , $l = 1$ mode at $\log(L/L_{\odot}) = 2.30$. The slightly longer time scales of the models used in this paper possibly are attributable to the fact that the Iben models are about one-half oxygen by mass and hence cool more quickly because of the slightly lower total heat capacity of the interior, in addition to the more careful treatment of Coulomb interactions in the Lamb (1974) equation of state. It is noteworthy that the evolutionary models of Iben, which are compositionally stratified, include nuclear shell burning, and treat shell flash phenomena explicitly, are considerably different from the simplified homogeneous models used here, yet they give strikingly similar results for the magnitude and sign of evolutionary period changes. In addition, we have investigated the pulsation properties of another set of PWD models produced by the evolution code that we used to prepare the starting models. These models contain compositionally stratified envelopes with hydrogen and helium layers, including nuclear shell sources, although they employ a somewhat simplified equation of state. This third $0.60 M_{\odot}$ sequence also showed pulsation properties similar to those discussed in § IV.

We can understand why these three sequences have such similarities by the following argument. The major differences between the three sequences are in their envelope structure when nuclear shell burning plays a role. For high-luminosity models, the period is largely determined in the interior of the star, below any nuclear shell sources. Therefore, at luminosities above the transition luminosity, the qualitative features of the pulsation properties for the three sequences reflect the basic similarities of their degenerate cores, with minor differences attributable to differences in core composition. By the time the models cooled below the transition luminosity of about $\log(L/L_{\odot}) = 2.0$, where the portions of the star near the surface begin to dominate the weight function, these differences in

envelope structure had begun to diminish as residual nuclear burning died away. Hence, the pulsation properties will remain somewhat similar even below the transition luminosity, despite differences in envelope composition and structure. The pulsation properties presented in this paper can therefore be considered representative of the entire class of theoretical PWD models.

Recently, Winget and collaborators determined dP/dt for the 516 s period of PG 1159–035. The reported value of dP/dt of $(-1.2 \pm 0.1) \times 10^{-11} \text{ s s}^{-1}$ corresponds to a time scale for period change of about 10^6 yr . This is in qualitative agreement with the time scales present in 0.60 and $0.78 M_{\odot}$ PWD models at $\log(L/L_{\odot}) < 2.2$. The high degree of degeneracy in standard post-PNN PWD models at the luminosity of the PG 1159 stars precludes any radius changes large enough to produce the negative value of dP/dt observed in PG 1159–035. One possibility is that this apparent discrepancy may, in fact, be attributable to our neglect of nonadiabatic effects on the pulsation period. For example, nonadiabatic effects most probably serve to decrease the period when the mode is unstable and the star is pulsating (W. D. Pesnell 1984, private communication). Evolution of the star into an instability strip will mean that the growth rate toward instability increases with time. If the adiabatic evolutionary period increase is small ($a \sim b$ in eq. [12]), then the observed value of dP/dt could reflect the nonadiabatic contributions to the period. Unfortunately, nonadiabatic analyses of *evolving* PWDs have not been performed thus far. In addition, if the star is rotating, conservation of angular momentum implies spin-up upon contraction, producing an additional contribution to b in equation (10) (Hansen, Cox, and Van Horn 1977). Simple dimensional analysis shows that this term can be important for rotation periods less than or the order of 2 hours. We are currently proceeding with an analysis of the effects of various rotation laws on dP/dt .

Other evolutionary considerations may also contribute to the observed sign of dP/dt . For example, a core composition heavier than carbon or oxygen would delay the onset of degen-

eracy in PNN models, and thus permit significant changes in radius at lower luminosities. We are currently investigating this possibility as well. Alternatively, different progenitors of PWDs can be considered; it is interesting to note that models appropriate to hot subdwarfs evolving along the “extended horizontal branch” (e.g., Greenstein and Sargent 1974) in the PG 1159 region of the H-R diagram (Wesemael *et al.* 1982) were used in WHVH and gave accurate estimates of the observed magnitude and sign of dP/dt for PG 1159–035. Even though the uncertainties in the luminosity of PG 1159–035 are large, we note that the possibility of adopting a luminosity of $\log(L/L_{\odot}) \geq 3.0$ for PG 1159–035 is unattractive. With such high-luminosity models, it would then be difficult to match the observed magnitude of dP/dt .

Observations of the other members of the class of pulsating PG 1159 stars are crucial to understanding the class properties. Specifically, it will be very interesting to learn whether the values of dP/dt for the other PG 1159 stars are similar to that of PG 1159–035 in both sign and magnitude. Such observations will enable us to determine whether nonadiabatic effects or the evolutionary status (or both) is responsible for the sign of dP/dt . In either case, this observable parameter will give us a new and powerful tool to aid us in understanding the nature of the pulsations of these stars and the state of PWD interiors.

We would like to thank J. P. Cox, I. Iben, W. D. Pesnell, and S. Starrfield for helpful discussions, and I. Iben and D. Hollowell for providing us with some of the PNN models of Iben (1984). We thank A. N. Cox for reading a draft of the manuscript and providing helpful comments that improved the presentation and augmented the scientific content of the paper. We also thank H. M. Van Horn for useful comments and G. Fontaine for his help in diagnosing the problems with the FGVH equation of state. This work was sponsored in part by McDonald Observatory and in part by the National Science Foundation, under grants AST 82-08046 through the University of Texas and AST 83-15698 through the University of Colorado.

REFERENCES

- Backus, G. E., and Gilbert, J. F. 1967, *Geophys. J.R.A.S.*, **13**, 247.
 Bond, H. E., Grauer, A. D., Green, R. F., and Liebert, J. 1984, *Ap. J.*, **279**, 751.
 Brickhill, A. J. 1975, *M.N.R.A.S.*, **170**, 404.
 Carroll, B. W. 1981, Ph.D. thesis, University of Colorado.
 Cox, J. P. 1980, *Theory of Stellar Pulsation* (Princeton: Princeton University Press).
 Cox, J. P., and Giulì, R. T. 1968, *Principles of Stellar Structure* (New York: Gordon & Breach).
 Deubner, F., and Gough, D. 1984, *Ann. Rev. Astr. Ap.*, **22**, 593.
 Dziembowski, W. 1971, *Acta Astr.*, **21**, 289.
 ———. 1977, *Acta Astr.*, **27**, 203.
 Epstein, I. 1950, *Ap. J.*, **112**, 6.
 Fontaine, G., Graboske, H. C., and Van Horn, H. 1977, *Ap. J. Suppl.*, **35**, 293 (FGVH).
 Goossens, M., and Smeyers, P. 1974, *Ap. Space Sci.*, **26**, 137.
 Green, R. F., and Liebert, J. W. 1979, in *IAU Colloquium 53, White Dwarfs and Variable Degenerate Stars*, ed. H. M. Van Horn and V. Weidemann (Rochester: University of Rochester), p. 118.
 Greenstein, J. L., and Sargent, A. I. 1974, *Ap. J. Suppl.*, **28**, 157.
 Hansen, C. J., Cox, J. P., and Van Horn, H. M. 1977, *Ap. J.*, **217**, 151.
 Iben, I., Jr. 1982, *Ap. J.*, **260**, 821.
 ———. 1984, *Ap. J.*, **277**, 333.
 Iben, I., Jr., and Tutukov, A. V. 1984, *Ap. J.*, **282**, 615.
 Kovetz, A., and Harpaz, A. 1981, *Astr. Ap.*, **95**, 66.
 Lamb, D. Q. 1974, Ph.D. thesis, University of Rochester.
 Lamb, D. Q., and Van Horn, H. M. 1975, *Ap. J.*, **200**, 306.
 McGraw, J. T., Starrfield, S. G., Liebert, J., and Green, R. F. 1979, in *IAU Colloquium 53, White Dwarfs and Variable Degenerate Stars*, ed. H. M. Van Horn and V. Weidemann (Rochester: University of Rochester), p. 377.
 Osaki, Y. 1975, *Pub. Astr. Soc. Japan*, **27**, 237.
 Osaki, Y., and Hansen, C. J. 1973, *Ap. J.*, **185**, 277.
 Paczyński, B. 1970, *Acta Astr.*, **20**, 47.
 ———. 1971, *Acta Astr.*, **21**, 417.
 ———. 1974, *Ap. J.*, **192**, 483.
 Schönberner, D. 1979, *Astr. Ap.*, **79**, 108.
 ———. 1981, *Astr. Ap.*, **103**, 119.
 ———. 1983, *Ap. J.*, **272**, 708.
 Schwank, D. C. 1976, *Ap. Space Sci.*, **43**, 459.
 Scuffaire, R. 1974, *Astr. Ap.*, **36**, 107.
 Sion, E., Liebert, J., and Starrfield, S. G. 1985, *Ap. J.*, submitted.
 Starrfield, S. G., Cox, A. N., Hodson, S. W., and Pesnell, W. D. 1983, *Ap. J. (Letters)*, **268**, L27.
 Starrfield, S. G., Cox, A. N., Kidman, R. B., and Pesnell, W. D. 1984, *Ap. J.*, **281**, 800.
 Unno, W., Osaki, Y., Ando, H., and Shibahashi, H. 1979, *Nonradial Oscillations of Stars* (Tokyo: University of Tokyo Press).
 Wegner, G., Berry, D. C., Holberg, J. B., and Forrester, W. T. 1982, *Bull. AAS*, **14**, 914.
 Wesemael, F., Green, R. F., and Liebert, J. 1982, *Bull. AAS*, **14**, 915.
 Wesemael, F., Winget, D. E., Cabot, W., Van Horn, H. M., and Fontaine, G. 1982, *Ap. J.*, **254**, 221.
 Winget, D. E. 1981, Ph.D. thesis, University of Rochester.
 Winget, D. E., and Fontaine, G. 1982, in *Pulsation in Classical and Cataclysmic Variable Stars*, ed. J. P. Cox and C. J. Hansen (Boulder: University of Colorado Press), p. 46.
 Winget, D. E., Hansen, C. J., and Van Horn, H. M. 1983, *Nature*, **303**, 781 (WHVH).
 Winget, D. E., Kepler, S. O., Robinson, E. L., Nather, R. E., and O'Donoghue, D. 1985, *Ap. J.*, **292**, 606.

CARL J. HANSEN: Joint Institute for Laboratory Astrophysics, University of Colorado, Boulder, CO 80309

STEVEN D. KAWALER and DONALD E. WINGET: Department of Astronomy, University of Texas, Austin, TX 78712